Kinetics of Desorption of Hexane from the Microporous Metal Organic Framework RPM 1

M. Smith,[*] J.T. Culp, [*] E. Bittner, [*] B. Parker, [#] J. Li, [#] B. Bockrath[*]

[*]National Energy Technology Laboratory

US Department of Energy

P. O. Box 10940

Pittsburgh, Pennsylvania 15236

[#]Department of Chemistry and Chemical Biology

Rutgers University

610 Taylor Road

Piscataway, New Jersey 08854

Abstract

The kinetics of desorption of hexane from the microporous metal framework RPM 1 has been studied using a pulse mass analyzer. In this method a small sample of organic liquid was injected into a heated carrier gas that passes through a packed bed of adsorbent. The change in mass of the bed with time was observed following the adsorption of the pulse. RPM 1 is a microporous material of the general formula $[M_3(bpdc)_3(bpy)] \cdot 4DMF \cdot H_2O$, where M is either Co or Zn, bpdc is biphenyl dicarboxylate and bpy is 4,4′-bipyridine. The pores are channels of larger supercages (11 x 11 x 5 Å) connected by smaller windows of approximately 8 Å diameter. The desorption of hexane was well represented by a combination of two first order processes. Activation energies determined for the two processes over a temperature range of 373 to 473 K were 56 and 63 kJ/mol for RPM 1 (Co). The two activation energies are similar to isosteric heats of adsorption measured independently in earlier work at corresponding coverages. Similar values were found for RPM 1 (Zn). The pulse mass analyzer was found to be an effective way to investigate the dynamics of adsorption processes.

Keywords: Metal Organic Framework, hexane, desorption, pulse mass analyzer, kinetics

Introduction

Microporous metal organic frameworks (MMOFs) have attracted considerable attention as adsorbents for light gases and small organic molecules. [1, 2] A wide array of structures is now available and the capability to custom design a structure to fit a required function is growing. MMOFs combine many favorable attributes needed for versatile engineered adsorbents including well defined crystalline structures of high surface area and well defined micropores. The variety of structures suggests many applications that now range from gas storage [3,4,5,6,7] to hosts for ship in the bottle synthetic reactions.[8] They may also function as catalysts [9] and hold promise as catalyst supports. Their ability to effect separations based on the steric requirements of molecular structures is now being exploited based on the wide choice of available pore sizes and shapes. An MMOF with a window and gallery type of pore structure has recently been shown to sharply discriminate linear C_4 and lower alkanes from higher or branched alkanes. [10a] In this case branched alkanes are excluded because they cannot traverse the windows, while longer linear alkanes are excluded because they cannot be accommodated within a single gallery.

Characterization that relates structure to function is required to help such molecular engineering efforts. To this end, characterization by the evaluation of adsorption isotherms and the measurement of adsorption kinetics for organic molecules [10] and small gas molecules [11] has already been used. Molecular simulations of the adsorption of alkanes in MMOFs have also provided valuable insights. [12, 13] Experimental information on the kinetics of adsorption or desorption would be a useful aid for the further development of these materials, but is not generally well developed.

Here we present a study of the kinetics of desorption of organic molecules from two related MMOFs by a novel experimental technique using a pulse mass analyzer. [14] The MMOFs studied, RPM-1-Co and RPM-1-Zn, are microporous materials of the general formula $[M_3(bpdc)_3(bpy)]\cdot 4DMF\cdot H_2O$, where M is either Co or Zn, bpdc is biphenyl dicarboxylate and bpy is 4,4′-bipyridine. [7, 8] The pores of these materials are channels of larger supercages (11 x 11 x 5 Å) connected by smaller windows with an aperture of approximately 7 x 8 Å. The utility of this joined supercage structure was effectively demonstrated by its use as a host in a “ship-in-the-bottle” synthesis. Photolysis of *o*-methyldibenzylketone held within the channels of RPM-1

proceeded with a cage effect of essentially 100% as a result of the confinement of the organic starting material within the pores. [8]

Study of the adsorption and desorption kinetics of organic vapors can give insight into rates of transport within the crystalline porous material and may serve as a useful adjunct to thermodynamic data obtained from traditional isotherms. [15a] The "Zero Length Column" (ZLC) chromatographic technique [15b] is a prominent example. In this method the kinetics of the desorption of vapors from a thin fixed bed of microporous adsorbent is used to obtain intra-particle diffusivities. Generally, the desorption kinetics are observed under high flow rate conditions after the supply of the adsorbed vapor has been cut off. Further development and theoretical treatment of carefully controlled, low-flow ZLC by Ruthven and coworkers [15c] demonstrated that a complete isotherm can be generated using this technique. In an extension of this chromatographic technique, Banas et al. used NMR to directly observe the decay of the concentration of the adsorbed vapor on the particles in the bed. [15d] Another and very convenient method for obtaining the kinetics of desorption by directly observing changes in the amount of adsorbed phase with a pulse mass analyzer is demonstrated here.

The pulse mass analyzer has been used previously to directly measure the change in the mass of material on an adsorbent with time under ZLC-like conditions [14]. This was a comparative study of the kinetics of the desorption of a series of organic vapors from single-walled carbon nanotubes. The instrument provides a direct measure of the change in mass as a pulse of organic vapor is carried through a small packed bed of adsorbent. Rate constants and activation energies may be extracted from the observed rise and fall of the mass curve resulting from the adsorption and desorption of the organic vapor of choice. Among other things, this method offers a relatively rapid and easy way to determine the activation energy for the desorption processes. A qualitative characterization of the physical and chemical nature of the pores may also be obtained. In the work reported here, the kinetics of desorption of hexane from RPM-1-Co are correlated to the isotherms and heats of adsorption obtained earlier.

Experimental

Materials

Hexane was 99+% pure obtained from Aldrich Chemical Company. Helium was Matheson Tri-Gas UHP grade (99.99 %) and was passed through a Matheson Gas Purifier

Cartridge Type 452 (4A molecular sieves) to remove traces of moisture. The MMOFs, $[Co_3(bpdc)_3(bpy)]\cdot 4DMF\cdot H_2O$ and $[Zn_3(bpdc)_3(bpy)]\cdot 4DMF\cdot H_2O$, were prepared as described earlier. [7, 8] $[Co_3(bpdc)_3(bpy)]\cdot 4DMF\cdot H_2O$ was synthesized by mixing $Co(NO_3)_2\cdot 6H_2O$ with bpdc and bpy in DMF in the molar ratio of 1:1.45:1.45:0.94. The reaction was carried out in a Teflon-lined autoclave and heated in an oven at 150 °C for 2 days. The product was filtered and washed with DMF (10 mL × 3 times) and dried at 80 °C for 3 hrs. $[Zn_3(bpdc)_3(bpy)]\cdot 4DMF\cdot H_2O$ was synthesized by reactions of $Zn(NO_3)_2\cdot 6H_2O$, bpdc and bpy in DMF in the molar ratio of 1:1:1:0.65. The same reaction and isolation conditions were used. Quantitative yields were obtained in both cases.

Instrumental

The pulse mass analyzer (PMA) has been used previously in a similar application. [14] The instrument (TEOM series 1500 Pulse Mass Analyzer manufactured by Rupprecht and Patashnick, Albany, NY) is a flow-through microbalance that detects mass changes by an inertial system that uses a vibrating tapered glass element enclosed within a stainless steel pressure vessel. The instrument is capable of operating from ambient temperature to 700 °C and from ambient pressure to 700 psia. The element is a hollow glass tube with a cylindrical sample bed, diameter 4 mm, height 6 mm, and a volume of 0.075 mL located at its lower end. Samples of about 30 mg of the adsorbent were packed into the bed between quartz wool plugs and retained there by a ventilated, gold-plated metal cap. The carrier gas stream passes through the packed bed while the sweep gas flows through the annular space between the element and the containment vessel. Gases were supplied from a manifold through mass flow controllers. Instrument control and data recording were managed through a PC system utilizing Labview© software programmed to control and record valve positions, the selection of the gases, their flow rates, system pressure and temperature, and other functions. The combined flow of both gas streams was sampled at the exit port by a capillary tube that serves as a transfer line to a quadrupole mass spectrometer (AMETEK MA 200).

During operation of the TEOM, changes in the mass of the sample bed are measured by recording changes in the frequency of oscillation of the tapered element. The element is stimulated to vibrate at its natural frequency (in the range of 40 cps) by a mechanical driver. The oscillation frequency is measured by an optical system that passes a beam of visible light

through two windows in the pressure vessel. Mass changes are determined by means of equation 1,

$$\Delta m = k(1/f_1^2 - 1/f_2^2) \qquad (1)$$

where f_1 and f_2 represent the frequencies observed at two different times, and k is an empirically determined constant. The frequency is measured at 0.8 second intervals and five second interval values are tabulated as a "Raw" data file. These are smoothed by a ten second running average process to give "ATM" values for mass change. These ATM values were used to fit the desorption kinetics. To determine the value of k, the instrument was equilibrated at the temperature and flow conditions to be used in the desorption experiment and the frequency of the empty reactor was measured with and without the retaining cap in place. The constant was calculated using the known mass of the cap. Since k changes in a complex way with temperature, all of the data in this study were acquired under isothermal conditions. Desorption kinetics were observed following a standard protocol for all experiments. The sample was loaded into the bed of the reactor and the He carrier gas and purge flows adjusted to their nominal values (50 mL/min).

Solvents incorporated during preparation of the MMOFs were removed by heating in a He stream to 180 °C for 1h for the Zn compound and to 150 °C for 48 h for the Co analog, following a regimen previously determined [7,8]. Stable baselines were reached eventually at the elevated temperature indicating volatile matter had completely left the sample. The mass loss in each case corresponded to that expected on the basis of previous TGA experiments [8]. The temperature was then changed to the experimental set point and time allotted for the baseline to become stable. A pulse of organic liquid was injected into the heated injector port with a 10μL syringe and the change in mass of the sample bed observed with time. An immediate increase in mass was followed by a gradual decrease as the sorbed material was desorbed. The mass was recorded as a running average every 5 seconds. Control experiments were performed without any adsorbent packed in the sample bed other than the quartz wool normally used as packing. In this case a just detectable increase in mass (10-20 μg) was observed during the passage of the pulse through the bed. This increase is attributed to the change in carrier gas density caused by the pulse of organic vapor. This change is negligible compared to those typically observed with

a sample of MMOF. Similar results were obtained when non-porous materials (salt, sand, glass beads) were packed in the bed. The identity and shape of the pulse was further confirmed by observation of the response of the mass spectrometer that sampled the tail gas from the instrument. The typical pulse width for a bed on inert material was found to be on the order of 5 secs. The rates of desorption measured here are much slower than the time required to sweep the bed and should represent a good approximation of the rate of intra- particle diffusion.

The experiments reported here have been carried out over a limited range of conditions. Full studies of the diffusional properties of similar beds of adsorbents show many factors can affect the rate of desorption. These factors include particle size, carrier gas flow rate, bed size, type of adsorption isotherm, and others. [15a] In this preliminary work, most of these variables were held constant to focus on the intrinsic properties of the MMOFs. A single packed bed was used for all experiments with either MMOF. A high gas flow rate was chosen to reduce the effect of interparticle diffusion. This flow rate corresponds to an exchange rate of more than 27 times the volume occupied by the sample every second. These provisions favor the dominance of the rate data by the inherent properties of the adsorbent. As described below, the close agreement that is found between the activation energies measured by these experiments and the independently measured isosteric heats of adsorption support this conclusion.

Results and Discussion

A typical growth and decay curve following a pulse of hexane on RPM-1-Zn is shown in Fig. 1. A rapid growth in mass is seen over a period of about 20 seconds. Since each of the data points represent a running 10 second average, the actual increase occurs even faster. Inspection of the mass change data before they were averaged led to an estimate that the growth curve is complete in about 5 seconds or less. The transit time for the entire pulse to pass through the sample bed under these flow conditions has been estimated by independent experiments to be approximately five seconds. [14] Shortly after reaching a maximum, a slow decay sets in corresponding to desorption of the retained material. The height of the mass curve represented roughly 40 to 75 % of the total amount of hexane injected, indicating that the MMOF captured a substantial fraction of the pulse. The decay curve then returned to baseline after a sufficiently long time, indicating that essentially all of the adsorbed material evolved from the bed of RPM-1.

The rate curves were analyzed over the time span from the end of the pulse to within 97% of return to baseline.

A rate law using a single first order equation for desorption was tested initially. A least squares fit of calculated mass to the experimental values at each time (t) was performed using Microsoft Excel Solver© using the expression, mass = ae^{-kt} , where a is the maximum mass at t = 0 and k is the first order rate constant for desorption. Good fits to data were obtained for those cases when the amount of hexane desorbed represented a relative small fraction of the saturated loading. This was seen with smaller than normal injection sizes (1 μL) or at temperatures high enough that only the rate of the desorption tail could be reliably measured. Larger injection sizes made at moderate temperatures were poorly described by a singe first order decay. In these cases it was clear from plots of the residuals such as illustrated in Fig. 2 that there was a significant deviation from experimental values in the early and late phases of the desorption. Further, the F test consistently indicated a low probability that the single desorption model correctly fits the data. We note that the higher loadings go beyond the Henry law region of the isotherms. A more complicated decay curve may thus be expected. A more detailed analysis of data that spans the region of nonlinear equilibrium conditions in high-flow ZLC experiments has been given. [15e,f] In this preliminary work we have not attempted to extract diffusion coefficients by adopting a particular model. Instead we simply find that curves from experiments at higher loadings can be well fit by inclusion of a second first order process. As discussed later, the kinetics of the two parts of the total desorption curve can be correlated with the change in isosteric heart of adsorption with coverage

Inclusion of a second first order process produced noticeably better fits and the histograms of the residuals seemed to be normal. A rate law of the form

$$\text{Mass}(t) = B + ae^{-k_1 t} + be^{-k_2 t} \qquad (2)$$

where B corrects for the non-zero baseline, a and b are the masses accounted for by the separate desorptions 1 and 2, and k_1 and k_2 are the rate constants, was generally satisfactory. The goodness of fit, as measured by Pearson R^2 values, was typically better than 0.999.

Close inspection of the initial portion of the decay (Fig 3) reveals that the shape of the curve near the maximum is somewhat irregular, tending to flatten before the characteristic shape

of the rest of the decay is established. We believe this is due to the competitive rates of adsorption and desorption that occur simultaneously during the period at the tail of the pulse. In cases at higher temperatures when desorption is very rapid the degree of flattening is not pronounced. In all cases, the decay kinetics were evaluated starting from the point just beyond the flat segment when only desorption was involved.

The decay curve beyond the time zone of mixed adsorption/desorption is well represented by the summation of two first order decay processes as illustrated in Fig. 4 (Note: For clarity, every tenth point is shown.) The red open circles are calculated values using equation (2). The experimental values are given by the blue line. The green triangles represent the contribution of $be^{-k_2 t}$, while the magenta squares are from $ae^{-k_1 t}$. To obtain the best representation of the bulk of the decay, the data used for fitting the curves were restricted to the interval of up to about 5 half lives for k_2. This point is indicated on the curve by the filled red circle. The rest of the curve (red open circles) indicates that the calculated values are good representations of the observed data when extrapolated well beyond the region actually used in the fit.

Replicate injections provided rate constants that were in close agreement. Deviations in k_2 estimated from three replicates were about 1 % of the value, while those for k_1 (the faster decay) were 9% of the values. In addition, comparisons were made using either a much smaller or a larger injection size. The fast decay portion was not evident with the smaller injection size (1μL) and the decay curve could be described by a single first order equation. The average value of k was within 4% of that of k_2 for the nominal injection size. When a larger injection size was used (7 μL) the pre-exponential "a" factor associated with the fast decay was markedly increased and the ratio of a/b decreased (see Table1). These observations are consistent with a sequential loading of adsorption sites. The proportion of hexane associated with the faster decay increases with greater loading whether caused by larger injection sizes or lower temperature. On the whole the observed desorption rate curves found at higher loadings can be adequately described by a combination of two first order processes..

Rate constants and coverages for the two RPMs are given in Table 1. The adsorption was sufficiently rapid so that a significant quantity of organic vapor was taken up during the passage of the pulse through the bed. The values may be compared with the saturation value of 150 mg/g reported from the isotherm for RPM-1-Co taken at 80 °C. Coverages reached during the pulse experiments range from 31 to 63 % of this value. For injections of the same size, the

maximum amount adsorbed decreased with rising temperature, as expected. Increasing the injection size by 3-5 times the nominal mass of hexane did not increase the value of b, the amount attributable to the slower desorption. On the other hand, the value for a is sensitive to injection size and was observed to go to zero for 1 μL injections at 473 K on the Co sample. Limitation to fuller coverage may be the result of a combination of slower diffusion of the organic vapor into the pores once they become partially filled with hexane and the short exposure times afforded by the injection technique. A previous kinetic experiment found that the initial rate of uptake of cyclohexane vapor by RPM-1-Co was rapid but that full saturation required sorption times on the order of tens of minutes. [8] This slow rate of equilibration was attributed to the relatively small dimensions of the pore windows.

The rate constants for the first segment of the desorption range from 3.6 to 8.2 times those of the second. There are some small differences between the results from the Zn and Co versions of the material. At the two common temperatures, the rate constants for the Zn material were somewhat higher than those for the Co analog. This difference was a factor of about 1.7 for k_1 and 1.3 for k_2. Small differences were also noted in the activation energy parameters as described below.

Decay curves for hexane were measured at several temperatures. The energies of activation extracted from the Arrhenius plots are recorded in Table 2. The values for the two MMOFs are very close as might be expected for materials that differ by substitution of Co for Zn and have very similar but not exactly the same crystal structure [7]. This may also indicate that the strength of the interaction with the sorbent, a hydrophobic and nonpolar material, is dominated by the organic linker rather than the metallic center. In addition, the pre-exponential factors were virtually identical for k_1 (Ln A = 12.3). For k_2, the value for the Zn analog was somewhat higher than for the Co analog (Ln A = 13.9 vs. 12.8).

The activation energies from the kinetic experiments may be compared with the single value of 66 kJ/mol measured previously for the isosteric heat of adsorption of hexane on RPM-1-Co. [8] This value is slightly higher and presumably reflects the strength found at very low coverage. In addition, re-examination of the previously published isotherms [8] showed that the isosteric heat decreased to 46 ± 6 kJ/mol at the higher coverage of 100 mg/g, a value slightly above the maximum coverages used in our rate studies. The isosteric heat at this loading is within experimental error of the E_{act} value for the faster desorption (56 ±5 kJ/mol (Table 2)). In

contrast to the thermodynamic value derived in reference to a single coverage from isotherms taken at various temperatures, the kinetic energy of activation refers to the range of coverages sampled over the desorption curve. In this light, the smaller values found for the activation energies may be a reflection of the decrease in isosteric heats of adsorption expected to occur as coverage increases.

The structure of the Zn and Co RPMs are closely similar in most parts but differ in the coordination of the metal ions. [7] This leads to differences in surface area, total pore volume, hydrogen storage capacity. The values for the Co structure are somewhat higher in all cases. In accord with this trend, the coverages achieved by injecting the same amount of hexane were also larger for the Co structure.

An indication of the strength of the physisorption interaction energy may be had by comparison to the heat of vaporization of n-hexane, 31.54 kJ/mol. [16] The activation energies approach twice this value and reflect a surprisingly strong interaction energy. Reference to the structure of RPM-1 provides some insight. The crystal structure derived from XRD shows a system of relatively flattened bottle-like pores connected by narrower necks with dimensions of about 7 by 8 Angstroms (Fig. 5). The narrow dimensions of the pores and especially the small diameter of the windows joining the pores likely play an important role in restricting removal of hexane from RPM-1.

Conclusions

We have found that the kinetics of desorption of a hexane from RPM-1 is well represented by a combination of two first order rate processes. This new kinetic data compares well with thermodynamic data obtained in a separate study of the same materials. The slower rate process is associated with desorption in the Henry law region of the isotherm. Addition of a second, faster desorption was found to be necessary when the loading went beyond the Henry law region. Activation energies were obtained for both the faster and slower processes. The values for the desorption of hexane from ROM 1 (Co) are close to the isosteric heats of adsorption measured at loadings similar to the ranges covered by the two desorption processes. The pulse technique using the TEOM is thus a valuable tool for the study of desorption kinetics for microporous adsorbents. A large number of compounds can be rapidly surveyed by this relatively simple technique. Kinetic studies of the adsorption and retention of low boiling compounds of various

sizes, shapes, and functionality preformed in this way can be used as an informative probe of the structure and surface of microporous materials. Further work is underway to exploit the pulse mass analyzer as an instrument for evaluating adsorption properties of a wide variety of MMOF and related materials.

Acknowledgements

This publication was supported in part by the appointment of MRS and EWB to the US Department of Energy Fossil Energy Faculty Research Program and JTC to the Postgraduate Research Participation Program at NETL administrated by Oak Ridge Institute for Science and Education. Reference in this work to any specific commercial product is to facilitate understanding and does not necessarily imply endorsement by the United States Department of Energy.

References

1. O. M. Yaghi, M. O'Keefe, N. W. Ockwig, H. K. Chae, M. Eddaoudi, J. Kim, Nature 423 (2003) 705.
2. R. Q. Snurr, J. T Hupp,.S. T. Nguyen, AIChE J. 50 (2004) 1090.
3. D. N. Dybtsev, H. Chun, S. H. Yoon, D. Kim, K. Kim, J. Am. Chem. Soc. 126 (2004) 32.
4. (a) S. S.-Y. Chui, S. M-F. Lo, J. P. H. Charmant, A. G. Orpen, I. D. Williams, Science 283 (1999) 1148. (b) A. Vishnyakov, P. I. Ravikovitch, A. V. Neimark, M. Bulow, Q. M. Wang, Nano Lett. 3 (2003) 713.
5. L. Pan, M. B. Sander, X. Y. Huang, J. Li, M. Smith, E. Bittner, B. Bockrath, J. K. Johnson, J. Am. Chem. Soc. 126 (2004) 1308.
6. J. L. C. Rowsell, A. R. Millward, K. S. Park, O. M. Yaghi, J. Am. Chem. Soc.126 (2004) 5666.
7. J.-Y. Lee, L. Pan, S. K. Kelly, J. Jagiello, T. J. Emge, J. Li, Adv. Mater. 17 (2005) 2703.
8. L. Pan, H. Liu, X. Lei, X. Huang, D. Olson, N. J. Turro, J. Li, Angew. Chem. Int. Ed. 42 (2003) 542.
9. K. Schlichte, T. Kratze, S. Kaskel, Micropor. Mesopor. Mater. 73 (2004) 81.

10. (a) L. Pan, D. H. Olson, L. R. Ciemnolonski, R. Heddy, J. Li, Angew. Chem. Int. Ed 45 (2006) 616. (b) L. Pan, B. Parker, X. Y. Huang, D. H. Olson, J.- Y Lee, J. Li, J. Am. Chem. Soc. 128 (2006) 4180. (c) A. J. Fletcher, E. J. Cussen, T. J. Prior, M. J. Rosseinsky, C. J. Kepert, K. M. Thomas, J. Am. Chem. Soc. 123 (2001) 10001. (d) A. J. Fletcher, E. J. Cussen, D. Bradshaw, M. J. Rosseinsky, K. M. Thomas, J. Am. Chem. Soc. 126 (2004) 9750.
11. (a) J. T. Culp, C. Matranga, M. Smith, E. W. Bittner, B. Bockrath, J. Phys. Chem. B. 110 (2006) 8325. (b) S. Natesakhawat, J. T. Culp, C. Matranga, B. Bockrath, J. Phys. Chem., C. 111 (2007) 1055.
12. L. Sarkisov, T. Duren, R. Q. Snurr, Mol. Phys.102 (2004) 211
13. J. Jiang, S. I. Sandler, Langmuir 22 (2006) 5702.
14. E. W. Bittner, M. R. Smith, B. C. Bockrath, Carbon 41 (2003) 1231.
15. (a) D. M. Ruthven, Principles of Adsorption and Adsorption Processes, John Wiley and Sons, New York, 1984. (15b) M. Eic, D.M. Ruthven, Zeolites 8 (1988) 40. (c) F. Brandani, D. Ruthven, C.G. Coe, Ind. Eng. Chem. Res. 42 (2003) 1451. (d) K. Banas, F. Brandani, D.M. Ruthven, F. Stallmach, J. Kärger, Magnetic Resonance Imaging 23 (2005) 227. (e) S.F. Zaman, K.F. Loughlin, S.S. Al-Khattaf Ind. Eng. Chem. Res. 44 (2005) 2027. (f) S. Brandani, Chem. Eng. Sci. 53 (1998) 2719
16. N. S. Osborne, D. C. Ginnings, J. Res. NBS 39 (1947) 453.

Table 1. Rate Constants and Covereages for Hexane Desorption.

T(K)	k_1, sec^{-1}	a, mg/g	k_2, sec^{-1}	b, mg/g	Coverage (a+b), mg/g
$Zn_3(bpdc)_3bpy$					
448	0.177	7.2	0.0235	40.3	47.6
423	0.0424	13.2	0.00775	43.3	56.7
398	0.0157	15.1	0.0026	46.7	61.5
373	0.00539	18.7	0.00065	50.9	69.4
$Co_3(bpdc)_3bpy$					
473	0.135	8.6	0.0369	41.1	49.6
423*	0.026	22.5	0.0056	65.1	87.7
373	0.00294	13.4	0.00051	81.0	94.3

* Injection size was 7μL (all others are 5μL)

Table 2. Activation Energies for hexane desorption.

RPM	E_{act}, kJ/Mole
RPM – Zn	
k_1	54.0 ± 5
k_2	66.0 ± 2.0
RPM - Co	
k_1	56.0 ± 5
k_2	63.0 ± 2.0

Figure captions.

Figure 1. PMA response to a 5 µl injection of n-hexane in helium carrier gas with RPM-1-Zn at 125 °C.

Figure 2. Residuals of the fit of a rate law using a single first order (a) and the sum of two first order processes (b). The distribution of residuals for the two part law is given in (c).

Figure 3. Expanded scale showing the time interval over a pulse of hexane on RPM-1-Zn at 125 °C.

Figure 4. Resolution of experimental decay curve for hexane desorption by summation of two first order processes.

Figure 5. Top: View of $[Zn_3(bpdc)_3bpy]\cdot 4DMF\cdot H_2O$ (**1**), showing 1D channels. Bottom: View of $[Co_3(bpdc)_3bpy]\cdot 4DMF\cdot H_2O$ (**2**) showing similar channels. Right: Estimated shape of 1D open channels. Solvent molecules (DMF and H_2O) are indicated in blue.

Fig. 1

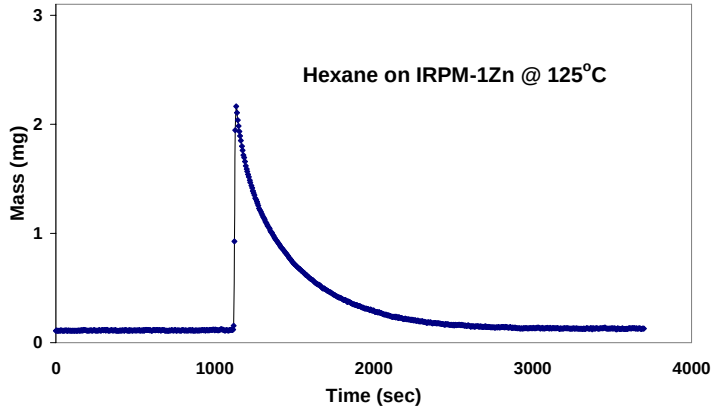
Hexane on IRPM-1Zn @ 125°C
Mass (mg)
Time (sec)
0
1
2
3
0
1000
2000
3000
4000

Fig 2.

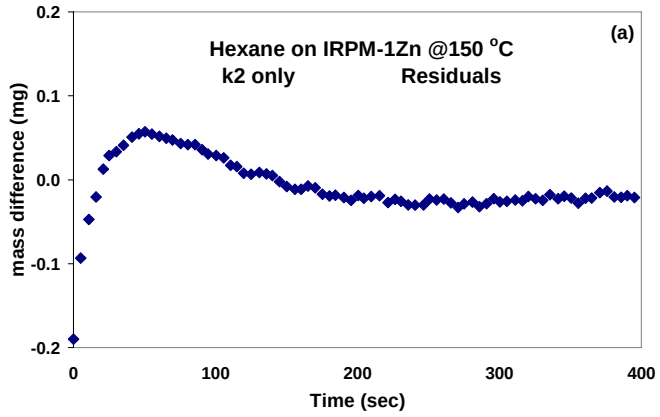
Hexane on IRPM-1Zn @150 °C
k2 only
Residuals
(a)
mass difference (mg)
Time (sec)
0.2
0.1
0.0
-0.1
-0.2
0
100
200
300
400

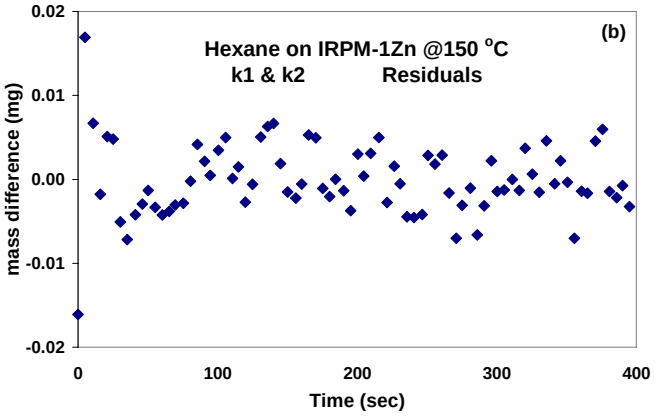
(b)
Hexane on IRPM-1Zn @150 °C
k1 & k2 Residuals
mass difference (mg)
0.02
0.01
0.00
-0.01
-0.02
0
100
200
300
400
Time (sec)

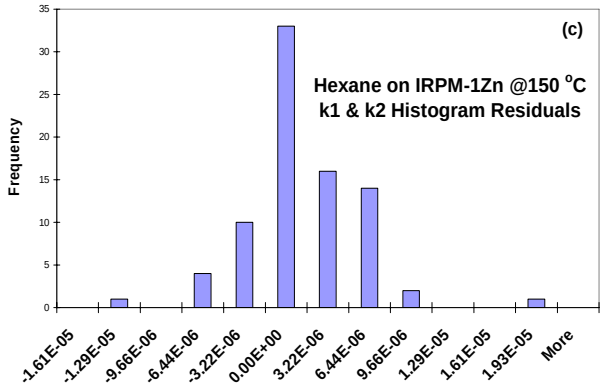
(c)
Hexane on IRPM-1Zn @150 °C
k1 & k2 Histogram Residuals
Frequency
35
30
25
20
15
10
5
0
-1.61E-05
-1.29E-05
-9.66E-06
-6.44E-06
-3.22E-06
0.00E+00
3.22E-06
6.44E-06
9.66E-06
1.29E-05
1.61E-05
1.93E-05
More

Fig. 3.

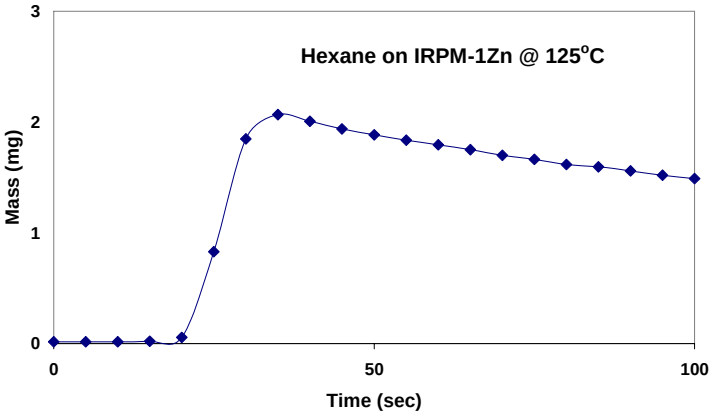
Hexane on IRPM-1Zn @ 125°C
Mass (mg)
3
2
1
0
0
50
100
Time (sec)

Fig 4.

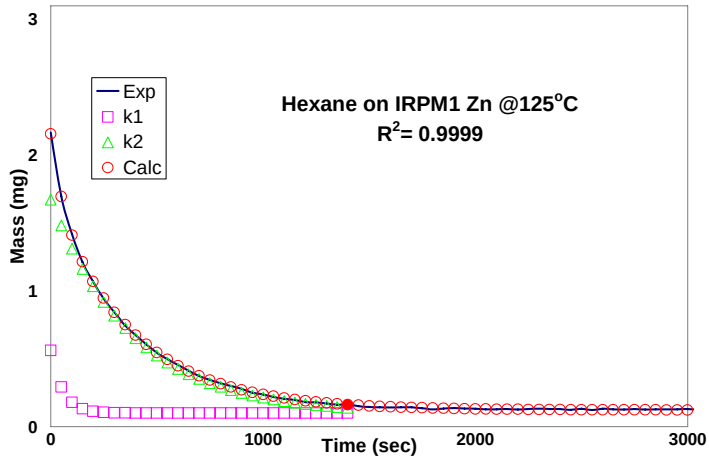
Exp
k1
k2
Calc
Hexane on IRPM1 Zn @125°C
R²= 0.9999
Mass (mg)
Time (sec)
0
1
2
3
0
1000
2000
3000

Fig. 5.

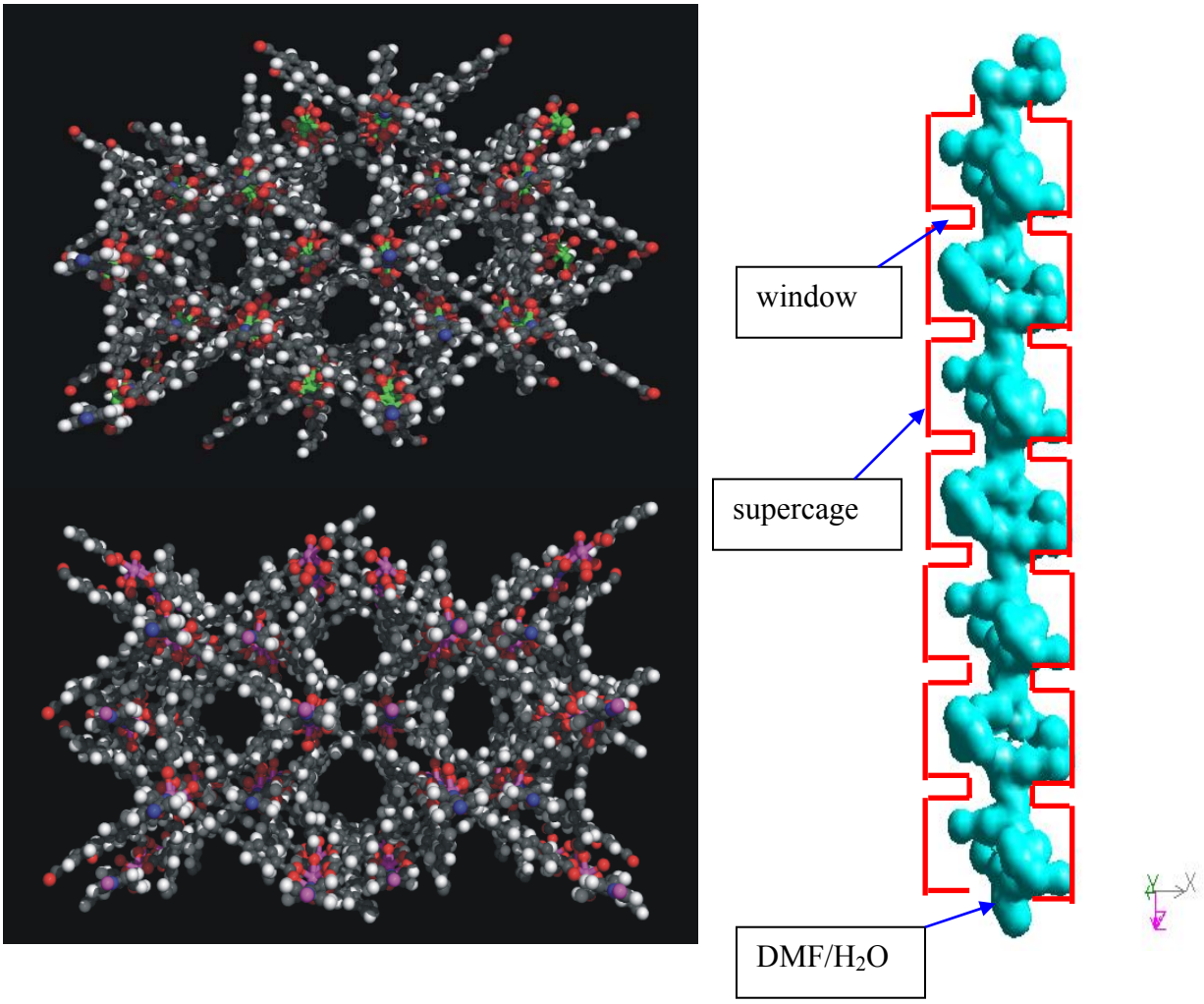
window
supercage
DMF/H2O